



## IN-SILICO MOLECULAR DOCKING OF DICHLOROFLOVAN FROM ZINGIER OFFICINALE AND ALLICIN FROM ALLIUM SATIVUM AGAINST MPRO A DRUG TARGET OF SARS COV-2

Mantri Sairam<sup>1</sup>, Chandini S Syed<sup>2</sup>, K Samuel John<sup>2</sup>, Amrutha V Audipudi<sup>2</sup>, Krishnaveni Ramakrishna\*<sup>3</sup>

<sup>1</sup>Vijaya Krishna Agro Food Processing Pvt Ltd, Remalle (V), Vijayawada, Andhra Pradesh, India

<sup>2</sup>Department of Microbiology, Acharya Nagarjuna University, Guntur, Andhra Pradesh, India

<sup>3</sup>Department of Microbiology, Vijayanagara SriKrishnadevaraya University, Ballari, Karnataka, India

\*Corresponding author: [krishnaveni@vskub.ac.in](mailto:krishnaveni@vskub.ac.in), [krishnaveni.chikkam@gmail.com](mailto:krishnaveni.chikkam@gmail.com)

Received: 07-12-2021; Revised: 05-04-2022; Accepted: 12-04-2022; Published: 30-04-2022

© Creative Commons Attribution-NonCommercial-NoDerivatives 4.0 International License <https://doi.org/10.55218/JASR.202213327>

### ABSTRACT

From decades, viral diseases including emerging and chronic viral infections are increasing worldwide health concern. Corona virus, SARS COV-2, is a new strain identified in 2019 caused Covid-19, in Wuhan, China has caused more than 5,304,772 infections and ~342,029 deaths worldwide over 203 countries, and the numbers are increasing exponentially from time to time. Since no specific treatment and diagnosis are available for COVID-19, discovery of new antiviral agents have become the most urgent need than in past, especially from natural sources. Hence, our present study is aimed to investigate bioactive molecules from *Zingiber officinale* (ginger) and *Allium sativum* (garlic) as potential SARS COV-2 main protease inhibitors, using a molecular docking by Auto dock 4.2, with the Lamarckian Genetic Algorithm, to analyze the probability of docking. SARS COV-2 main protease was docked with five selected compounds (zingerone, gingerol, paradol, dichloro flavin (ginger), and allacin (garlic), and were analyzed by Auto dock 4.2, PyMol version 1.7.4.5. Chloroquine and hydroxy chloroquine were used as standards for comparison. The binding energies obtained from the docking of Covid-19 main protease with biological ligand; zingerone, gingerol, paradol, dichloro flavin, and allacin were -5.31, -4.73, -5.51, -6.05, -3.74 kcal/mol, while, standard drugs such as hydroxy chloroquine and chloroquine possess binding energies of -4.88 and -5.25 kcal/mol respectively. It indicates that, zingerone, paradol and dichloroflavan show more binding energy than chloroquine and hydroxy chloroquine, whereas, gingerol and allacin exhibited lesser binding energy. Comparing these five molecules, dichloroflavan and paradol from ginger shows highest affinity and binding sites for target protein.

**Keywords:** Docking, Covid-19, Ginger-garlic, Chloroquine, Flavin, Allacin.

### 1. INTRODUCTION

There is an urgent need for novel and more effective antiviral drugs due to the global disease burden caused by Corona viral infections. During the search for natural drugs, medicinal herbs and their bioactive constituents became the center of interest, since they may provide feasible treatment options for the population of developing countries, where the majority of the population cannot afford for expensive chemical drugs of western medicine. Now-a-days viral infections are becoming a great threat to humans and often cause deaths worldwide [1]. Though viruses are composed of nucleic acids and protein coat, and an envelope (in case

of enveloped viruses), due to the metabolic properties of viruses, it is difficult to control them and there are still relatively few drugs for treatment of viral diseases. The major problem encountered in the treatment against viruses is their rapid adaptation and development of drug-resistance as well as the emergence of new hybrid viruses [2].

A Corona virus (Co-Vs) is a one such etiologic agent of severe infections in both humans and animals, which can cause disorder not only in the respiratory tract but also in the digestive tract leading to multiple organ failure. Previous studies of Co-Vs have reported that, Co-Vs can infect certain species of animals, including mammals,

avian species, and reptiles [3]. The new strain of Co-V was identified at the end of 2019, initially named 2019-nCoV, and emerged during an outbreak in Wuhan, China. Currently, no specific therapies for COVID-19 are available and investigations regarding the treatment of COVID-19 are lacking. However, the measures that have been implemented remain limited to preventive and supportive therapies, designed to prevent further complications and organ damage [4, 5]. As the world awaits eagerly for a therapy to combat COVID-19 virus (SARS-CoV-2) or (2019-nCoV), there have been several attempts that were made with several existing solutions and compounds to address the spectra of COVID-19 [6]. Alternative coronaviral targets include the spike protein (S), RNA-dependent RNA-polymerase (RdRp, nsp12), NTPase/helicase (nsp13) and papain-like protease (PLpro, part of nsp3) [7-15]. However, Viral proteases are well validated drug targets that have led to various approved drugs, for example, against chronic infections with human immunodeficiency virus (HIV) or hepatitis C virus (HCV), which employ aspartyl and serine proteases, respectively [16]. Meanwhile, efforts have been initiated to examine the potential of several metabolites from nature (herbs) in inhibiting the COVID-19 main protease (M-pro) using molecular docking analysis to arrive at binding affinity [17]. Khaerunnisa *et al.* [18] showed that several plant secondary metabolites such as kaempferol, quercetin, luteolin-7-glucoside, demethoxycurcumin, naringenin, apigenin-7-glucoside, oleuropein, curcumin, catechin, and epicatechin-gallate have the potential to inhibit the COVID-19 main protease. In a more recent paper, first released on 20 March 2020, Zhang *et al.* [15] reported a potent ketoamide inhibitor of COVID-19 main protease (M-pro) and suggest that it is subject to further investigation, it could form an attractive drug candidate [12, 17, 19, 20].

In this study, we examine the binding energy of ligands from ginger and garlic to COVID-19 main protease, as most of them are the internal integral part of the household kitchen and many cuisines, both Indian and other countries.

The rapid purpose of this study is to investigate the potentiality of these bioactive molecules to inhibit the proteins of COVID-19. Considering the fact that, most of the natural product ligands chosen for the study occur in commonly used spices [21]. It is likely that their eventual deployment as drug candidates could hasten regulatory approvals. Finally our studies, as evident from the results presented below, show that indeed,

few of the natural products ligand have acceptable binding affinity with COVID-19 main protease and compare well with a known predicted Covid drugs chloroquine and hydroxy chloroquine.

## 2. MATERIAL AND METHODS

### 2.1. Macromolecule preparation

Crystallographic protein structure of Covid-19 main protease was retrieved from protein data bank (PDB). Identification of active site of these proteins was done by using auto ligand and was visualized using the molecular graphics program PyMol® software [22, 23]. Macromolecule which is downloaded in the PDB format was energy minimized using Swiss PDB version v4.1 [24]. Before protein preparation, the macro molecule was prepared for docking by deletion of all water molecules, B and C side-chains and it was saved as PDB format. Polar hydrogens, Kollman and gasteiger charges were added to the macromolecule and saved it in a PDBQT format for docking purpose [25, 26].

### 2.2. Ligand preparation

Molecular structures of ginger (zingiberone, gingerol, paradol, dichloro flavin) and garlic (allicin) compounds were sketched using Marvin Sketch Software version 20.11.0 and the crystallographic structures of the standard drugs of chloroquine and hydroxy chloroquine were retrieved from the drug bank. Both the drug structures were generated in PDB File format followed by subsequent generation of their 3-D structures by using PyMol® software. Ligands were prepared for docking by choosing root and torsions [5, 27].

### 2.3. Docking studies

Macromolecule and ligand interactions were determined by Molecular Graphics Laboratory (MGL) tools of auto dock version 4.2 [28] and PDB files were converted to PDBQT files. The pre calculated grid maps at the size of 100, 110, 100Å (x, y, z) were used to include all the amino acid residues that are present in the receptor were done with the generated PDBQT files of macro molecule and ligand, using 0.375 angstroms as a grid space between points. Lamarckian genetic algorithm (LGA) used to chosen and confirm maximum of 10 conformers which were required for the docking process with 150 individuals as the population. Default settings of auto dock were used for the rest of the parameters. At the end of docking, the best poses/positions were analyzed for hydrogen bonding, binding energy/energies and root mean square (RMS)

calculations using PyMOL software. Intel CORE™ i3, 64 bit Operating System and 4GB RAM in DELL Windows 10 Laptop were used to complete the docking studies [29].

### 3. RESULTS

Three-dimensional structures of COVID-19 main protease (Pub med ID: 6LU7) from protein data bank (PDB), chloroquine, hydroxy chloroquine were retrieved from drug bank (DB00608; DB01611) and sketched ligand structures (zingerone, gingerol, paradol,

dichloroflavan and allicin) using Marvin Sketch, visualized in PyMol and were presented in Fig. 1.

#### 3.1. Active site identification on COVID-19 main protease

The amino acids that are present in the active site of protein 6LU7 are LYS- Lysine, SER- Serine, VAL- Valine, ASP- Aspartic acid, ASN- Asparagine, THR- Threonine, PHE- Phenyl Alanine, ILE- Iso leucine, GLN- Glutamine, TYR- Tyrosine, ARG- Arginine, ASP- Aspartic acid were identified by using auto ligand software and shown in Table 1.

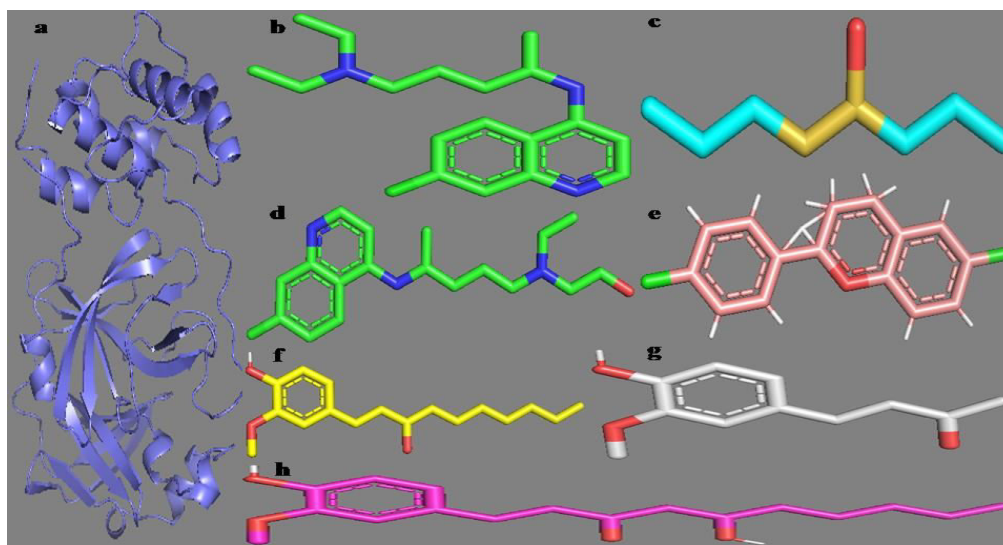


**Fig. 1: Three dimensional structures of protein and ligands; a) Covid-19 main protease; b) Chloroquine; c) Allicin; d) Hydroxy chloroquine; e) Dichloroflavan; f) Paradol; g) Zingerone; h) Gingerol**

**Table 1: Amino acids present in the active sites of macro molecules**

Macro molecule	Residues	Amino acids
Covid19 main protease	102, 158, 104, 152, 151, 111, 292, 106, 292, 110, 107, 239, 237, 131, 289	LYS, SER, VAL, ASP, ASN, THR, PHE, ILE, THR, GLN, GLN, TYR, TYR, ARG, ASP

#### 3.2. Molecular docking

About 10 runs were performed to obtain the best docking pose based on their docking score list of the ligand. After the completion of docking simulations, the macromolecule and ligand interactions were observed in terms of binding energy, number of hydrogen bonds, number of binding sites and the length of hydrogen bonds were given in Table 2.

##### 3.2.1. Chloroquine interaction with Covid-19 main protease

Interaction of chloroquine ligand with Covid-19 main protease by docking simulations produces the

conformers with a single cluster of 2.0 Å out of 10 docking runs with RMS-tolerance. The ligand shows highest binding energy -5.25 kcal/mol and the reference RMS value is 67.1. The ligand interacts with the two hydrogen bonds that occur at THR292 and GLN110 on the active site of protein with the bond lengths of 2.82Å. Out of the two amino acids, THR292 acts as a binding site, as shown in Table 2 & Fig. 2.

##### 3.2.2. Hydroxy chloroquine interaction with covid-19 main protease

Interaction of hydroxy chloroquine ligand with Covid-19 main protease by docking simulations produces the

conformers with a single cluster of 2.0 Å out of 10 docking runs with RMS-tolerance. The ligand shows highest binding energy -4.88 kcal/mol and the reference RMS value is 61.98. The ligand interacts with the three

hydrogen bonds that occur at MET276, ASN277 and GLY279 on the active site of protein with the bond length of 2.95Å. Out of three amino acids, GLY278 acts as a binding site, as given in Table 2; Fig. 3.

**Table 2: Covid-19 main protease protein interaction with different ligands**

Ligand Molecule	No. of H-bonds	Length of H-bond (Å)	Binding energy (kcal/mol)	Ligand efficiency	Inhibition constant $k_i$ ( $\mu$ M) at temperature (298.15K)	Total intermolecular energy (kcal/mol)	Reference RMS
Chloroquine	3	2.82	-5.25	-0.24	142.74	-6.74	67.1
Hydroxy chloroquine	3	2.95	-4.88	-0.21	265.92	-7.56	61.98
Dichloroflavan	1	3.16	-6.05	0.34	36.32	-6.35	62.77
Paradol	4	3.15	-5.51	-0.28	92.17	-8.79	72.72
Zingerone	4	2.03	-5.31	-0.38	128.81	-6.8	79.98
Gingerol	8	2.8	-4.73	-0.23	341.65	-8.31	69.94
Allicin	2	2.85	-3.74	-0.42	1.8	-5.24	53.02

\*Only lowest hydrogen bond length was given in the table

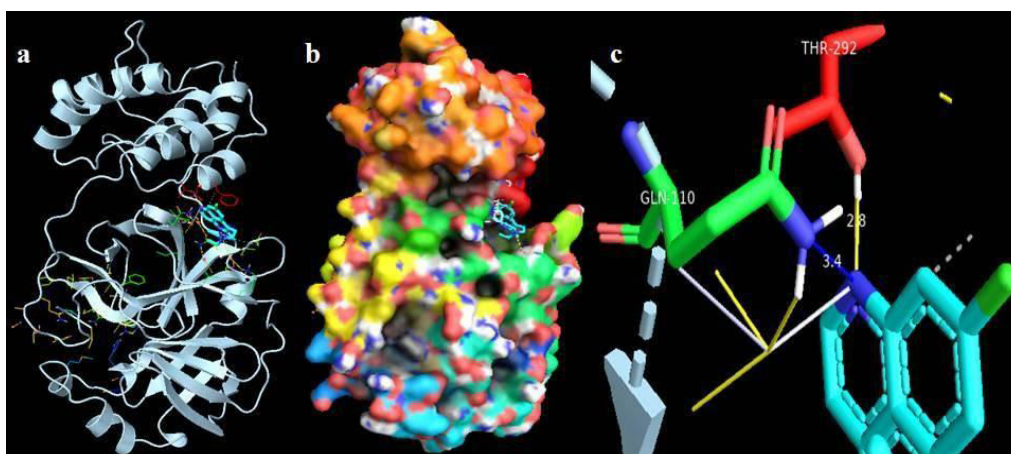


**Fig. 2: a) Covid-19 main protease docked by chloroquine showing interactions (ligand as cyan sticks); b) Best bind pose in the pocket of protein (showing ligand as cyan sticks) c) Amino acids involved in interaction (showing ligand as cyan sticks)**

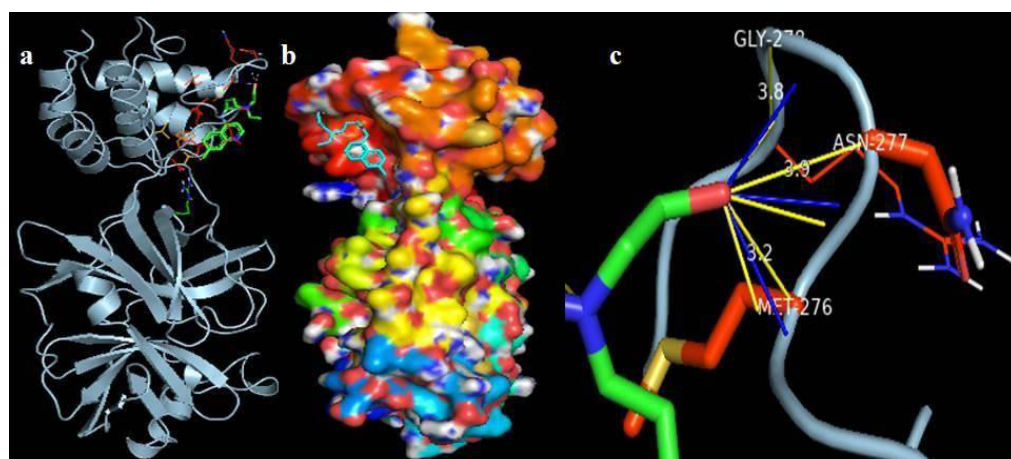


**Fig. 3: a) Covid-19 main protease docked by hydroxy chloroquine showing interactions (ligand as green sticks); b) Best bind pose in the pocket of protein (showing ligand as cyan sticks) c) Amino acids involved in interaction (showing ligand as green sticks)**

### 3.2.3. Dichloroflavan interaction with covid-19 main protease

Interaction of dichloroflavan ligand with Covid-19 main protease by docking simulations produces the conformers with a single cluster of 2.0 Å out of 10 docking runs with RMS-tolerance. The ligand shows

highest binding energy -6.05 kcal/mol and the reference RMS value is 62.77. The ligand interacts with the two hydrogen bonds that occur at LEU287 on the active site of protein with the bond lengths of 3.16Å (Fig 3A) and acts as a strong binding site, as shown in Table 2; Fig. 4.

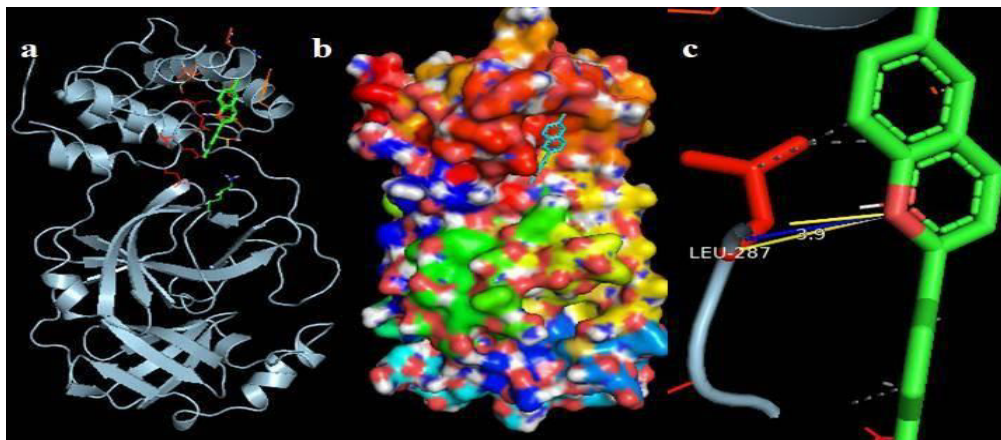


**Fig. 4:** a) Covid-19 main protease docked by dichloroflavan showing interactions (ligand as green sticks); b) Best bind pose in the pocket of protein (showing ligand as cyan sticks) c) Amino acids involved in interaction (showing ligand as green sticks)

### 3.2.4. Paradol interaction with covid-19 main protease

Interaction of paradol ligand with Covid-19 main protease by docking simulations produces the conformers with a single cluster of 2.0 Å out of 10 docking runs with RMS-tolerance. The ligand shows highest binding energy -5.51 kcal/mol and the reference RMS value is 72.2. The ligand interacts with the four hydrogen bonds which occur at TYR54, LEU141, GLY143 and GLN189 on the active site of protein with the bond lengths of 3.15Å. Out of four amino acids, GLN143 acts as a binding site, as shown in Table 2; Fig. 5.

### 3.2.5. Zingerone interaction with covid-19 main protease

Interaction of zingerone ligand with Covid-19 main protease by docking simulations produces the conformers with a single cluster of 2.0 Å out of 10 docking runs with RMS-tolerance. The ligand shows highest binding energy -5.31 kcal/mol and the reference RMS value is 79.98. The ligand interacts with the four hydrogen bonds that occur at TYR54, GLU166, THR190 and GLN192 on the active site of protein with the bond lengths of 2.03Å. Out of four amino acids, GLU166 acts as a binding site (Table 2; Fig. 6).

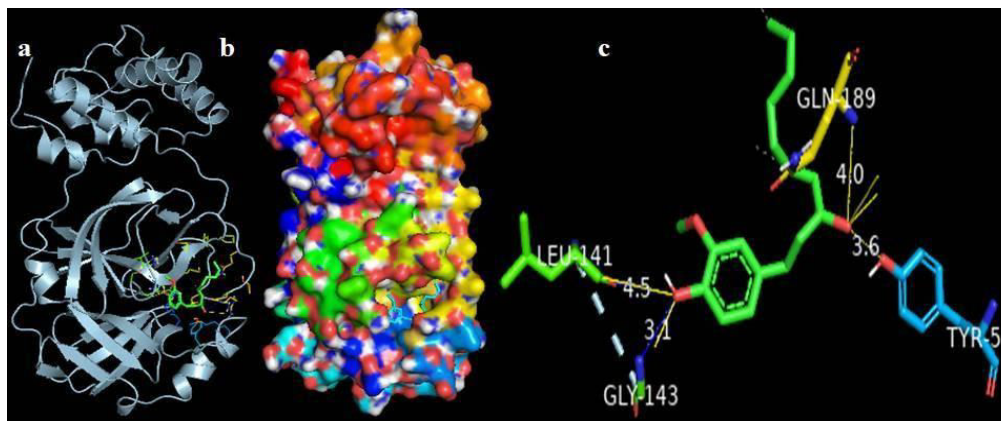


**Fig. 5:** a) Covid-19 main protease docked by paradol showing interactions (ligand as green sticks); b) Best bind pose in the pocket of protein (showing ligand as cyan sticks) c) Amino acids involved in interaction (showing ligand as green sticks)

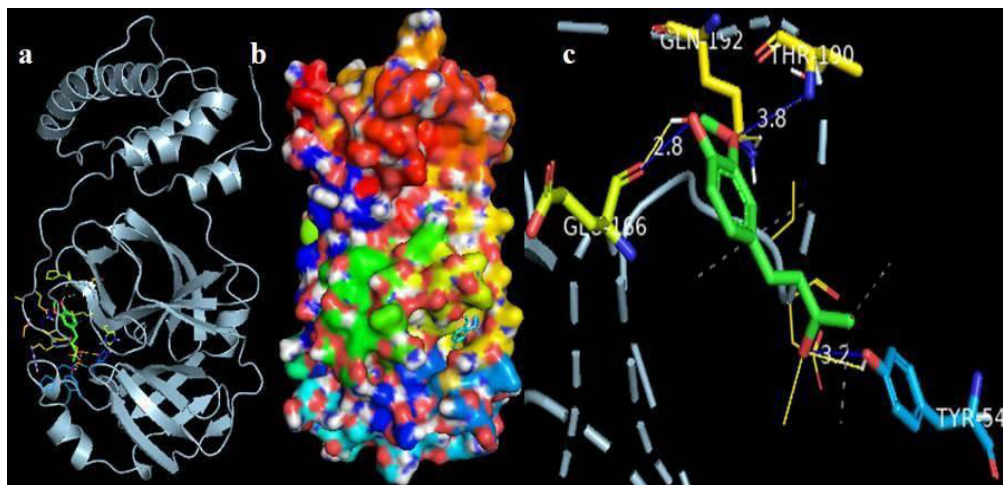


**Fig. 6:** a) Covid-19 main protease docked by zingerone showing interactions (ligand as green sticks); b) Best bind pose in the pocket of protein (showing ligand as cyan sticks) c) Amino acids involved in interaction (showing ligand as green sticks)

### 3.2.6. Gingerol interaction with covid-19 main protease

Interaction of gingerol ligand with Covid-19 main protease by docking simulations produces the conformers with a single cluster of 2.0 Å out of 10 docking runs with RMS-tolerance. The ligand shows highest binding energy -4.73 kcal/mol and the reference RMS value is 69.94. The ligand interacts with the eight hydrogen bonds occurring at LYS102, GLN110, THR111, ASP153, ASP153, SER158, THR292 and PHE294 on the active site of protein with the bond lengths of 2.8Å. Out of eight amino acids, GLN110, SER158 and THR292 acts as a binding site (Table 2; Fig. 7).

### 3.2.7. Allicin interaction with covid-19 main protease

Interaction of allicin ligand with Covid-19 main protease protein by docking simulations produces the conformers with a single cluster of 2.0 Å out of 10 docking runs with RMS-tolerance. The ligand shows highest binding energy -3.74 kcal/mol and the reference RMS value is 53.02. The ligand interacts with the two hydrogen bonds occurring at ARG4 and LYS5 on the active site of protein with the bond lengths of 2.85Å. Out of the two amino acids, LYS5 acts as a binding site as depicted in Table 2; Fig. 8.

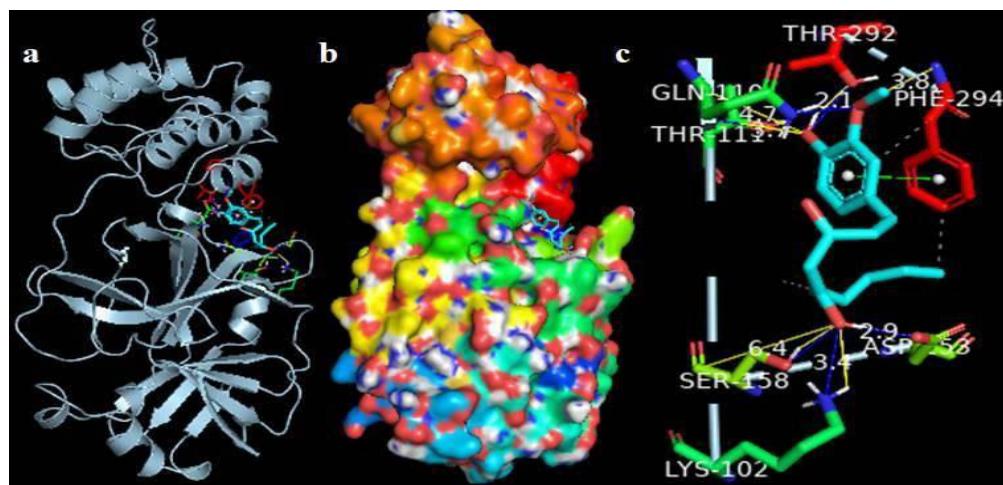


**Fig. 7:** a) Covid-19 main protease docked by gingerol showing interactions (ligand as cyan sticks); b) Best bind pose in the pocket of protein (showing ligand as cyan sticks) c) Amino acids involved in interaction (showing ligand as cyan sticks)

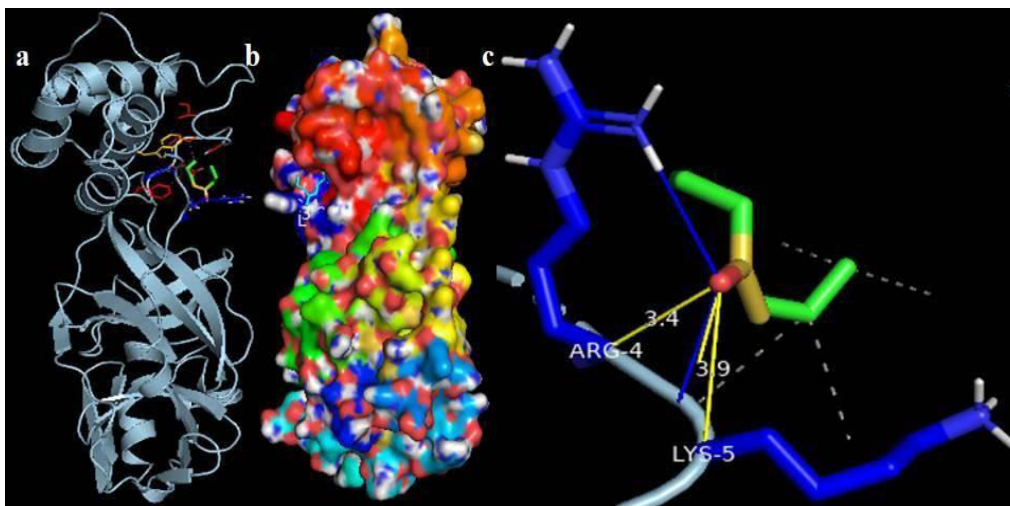


**Fig. 8: a) Covid-19 main protease docked by allicin showing interactions (ligand as green and yellow sticks); b) Best bind pose in the pocket of protein (showing ligand as cyan sticks) c) Amino acids involved in interaction (showing ligand as green and yellow sticks)**

#### 4. DISCUSSION

In this study, we have considered a total of 5 different extracts from (ginger-4 and garlic-1) of Indian medicinal herbs. Fig. 1 displays the molecular structures of a macromolecule (Covid-19 main protease), standard drugs and ligands (chloroquine, hydroxy chloroquine, dichloroflavan, paradol, zingerone, gingerol and allicin) extracted from these herbs. We have focused on mainly those compounds which have been found to possess anti-malarial, anti-viral or other biological activities. Gingerol (C<sub>17</sub>H<sub>26</sub>O<sub>4</sub>), zingerone (C<sub>11</sub>H<sub>14</sub>O<sub>13</sub>), paradol (C<sub>14</sub>H<sub>26</sub>O<sub>3</sub>), 4, 5, dichloroflavan (C<sub>15</sub>H<sub>12</sub>CL<sub>2</sub>O) were extracted from the ginger and allicin (C<sub>6</sub>H<sub>10</sub>S<sub>2</sub>) was extracted from garlic.

In order to compare the biological activity and pharmacological behavior of the extracted compounds, we have docked all the extracts with Covid-19 main protease and compared the results with the standards.

The molecular docking studies explore the interaction mechanism between ligands and receptors. The interactions between a ligand and receptor play a crucial role in the field of drug discovery. The molecular docking calculations have been performed as blind, i.e., covered the entire protein surface, not any specific region of the protein as the binding pocket in order to avoid sampling bias. The docking parameters such as binding energy, ligand efficiency, H-bond, bond-length along with amino acids (residue) found in the binding site pockets (active site) of Covid-19 main protease are listed in Table 1 and Table 2.

The binding energy (Kal/mol) of (drug) compounds depends on the type of bonding (H-bond) that occur

with the active site of the protein. The docking results in terms of binding energy shows that, dichloroflavan extract forms the highest binding energy of -6.05Kal/mol followed by paradol -5.51 Kal/mol, zingerone with -5.31 Kal/mol, gingerol with -4.73 Kal/mol and allicin -3.74 Kal/mol. When compared to the extracts, standard drug chloroquine forms the binding energy of -5.25Kal/mol which is lower than that of dichloroflavan, paradol, zingerone and higher than gingerol and allicin. Whereas the hydroxy chloroquine forms binding energy of -4.88 Kal/mol which is lower than dichloroflavan, paradol, zingerone and higher than gingerol and allicin. Based on the binding energy, the extracts can be ranked as; Dichloroflavan > paradol > zingerone > chloroquine > hydroxy chloroquine > gingerol > allicin. When compared with the standards in terms of number of hydrogen bonds, gingerol formed 8 which is highest of all the extracts followed by both zingerone and gingerol formed 4 hydrogen bonds each, allicin formed two hydrogen bonds and dichloroflavan forms a single hydrogen bond. When compared to the extracts, standard drug chloroquine forms 2 hydrogen bonds which is lower than gingerol, zingerone, paradol, and equals to allicin and higher than dichloroflavan when compared to the extracts. Standard hydroxy chloroquine forms 3 hydrogen bonds which are lower than gingerol, zingerone, paradol and higher than allicin and dichloroflavan. Based on the number of hydrogen bonds formed, the extracts can be ranked as; gingerol > zingerone > paradol > hydroxy chloroquine > chloroquine > allicin > dichloroflavan.

Avanish marvel, (2021) states that, compounds from ginger (gingerol) and garlic (allin) shows good binding efficiency of -6.957 and -6.461. According to Pandey, (2020), gingerol and paradol was docked against 6LU7 and shows the binding energies of -4.27Kal/mol and -5.16Kal/mol. similar results are compared in terms of binding sites, gingerol forms 3 binding sites followed by zingerone, paradol, dichloroflavan and allicin formed one binding site each. When compared to the extracts, standard chloroquine, forms 2 binding sites which is lower than gingerol and the highest among rest of all extracts. Whereas hydro chloroquine forms 3 binding sites which is equal to gingerol and the highest among rest of the extracts. Based on the number of binding sites formed, the extracts along with standards can be ranked as; hydroxy chloroquine=gingerol > chloroquine > zingerone > paradol >> allicin > dichloroflavan. By conducting *in silico* docking studies to inhibit the Covid-19 main protease by the extracts of Indian herbs (ginger and garlic), we noticed that the extracts possess inhibitory properties to a certain extent. Based on the binding energy, dichloroflavan appear as the most powerful inhibitor among the other extracts. The inhibition potentials of all these extracts were found to be larger than those of chloroquine and hydroxy chloroquine. These two anti-malarial drug compounds are already reported to inhibit Covid-19 main protease *in vitro*. Due to inherent toxicity and side-effects, however, they are not approved in most of the countries.

## 5. CONCLUSION

Our findings become very interesting towards the development of alternative (herbal) medicines having no apparent side-effects. Hence there is a need for further intensive research such as *in-vivo* trails to carry forward these findings and to downstream the products which are beneficial to mankind.

## 6. ACKNOWLEDGMENTS

Second author gratefully acknowledges the funding support provided by the Department of Science and Technology (DST), Ministry of Science and Technology, Government of India, New Delhi, under Inspire Fellowship- JRF (No.DST/INSPIRE Fellowship/2015/IF150034).

## Declaration of interest

The authors report no conflicts of interest

## 7. REFERENCES

1. Aanouz I, Belhassan A, El-Khatabi K, Lakhli T, El-Idrissi M, Bouachrine M. *J. Biomol. Struct*, 2020; **31**:1–9.
2. Agbowuro AA, Huston WM, Gamble AB, Tyndall JD. *A. Med Res Rev*, 2018; **38**(4):1295–1331.
3. Avinash M, Mukesh M, Gaur R K. *Defence Life Science J*, 2021; **6**(1):56-62.
4. Banerjee A, Kulcsar K, Misra V, Frieman M, Mossman K. *Viruses*, 2019; **11**: 41.
5. Berman HM, Battistuz T, Bhat TN, Bluhm WF, Bourne PE, Burkhard TK et al; *Acta Crystallogr*, 2002; **58**:899–907.
6. David G, Danka B, Sahdeo P, Amit K. Tyagi., *Frontiers in Microbiology*, 2016; **7**:1394.
7. Giménez BG, Santos MS, Ferrarini M, Fernandes JP. *Die Pharmazie*, 2010; **65**:148–152.
8. Grosdidier A, Zoete V, Michielin O. *Nucleic Acids Res*, 2011; **39**:270–277.
9. Harris R, Olson AJ, Goodsel DS. *Proteins: Struct,Funct,Bioinf.*, 2007; **70**:1506–1517.
10. Hilgenfeld R, Peiris M. *Antiviral Res*, 2013; **100**(1):286–295.
11. Khaerunnisa S, Kurniawan H, Awaluddin R, Suhartati S, Soetjipto S. *Preprints*, 2020;202003.0226.
12. Kim S, Thiessen PA, Bolton EE, Chen J, Fu G, Gindulyte A et al. *Nucleic Acids Res*, 2015; **44**:1202–1213.
13. Li G, De Clerc QE. *Nat Rev Drug Discov*, 2020; **19**(3):149–150.
14. Lipinski CA, Lombardo F, Dominy BW, Feeney P. *J. Adv. Drug Deliv Rev.*, 2012; **64**:4–17.
15. Lurie N, Saville M, Hatchett R, Halton J. *N Engl J. Med*, 2020; **382**(21):1969–1973.
16. Malik Y. S., Sircar S., Bhat S., Sharun K., Dhama K., Dadar M et al. *VetQ*, 2020; **40**:68–76.
17. Morris GM, Huey R, Lindstrom W, Sanner MF, Belew RK, Goodsell DS et al. *J. Comput. Chem*, 2009; **30**:2785–2791.
18. Noble S, Faulds D. *Drugs*, 1996; **52**(1):93-112.
19. Paules CI, Marston HD, Fauci AS. *JAMA*, 2020; **323**:707.
20. Pratibha P, Divyanshi S, Fahad K, Mohd A. *Biointerface research in applied chemistry*, 2021; **11**(4):11122-11134.
21. Sachan KRA, Kumar S, Kumari K, Singh D. *Worldwide*, 2018; **6**(3):116-112.
22. Salzberger B. *Der Internist*, 2006; **47**:1245-1250.
23. Sanner MF. *J. Mol. Graph*, 1999; **5**(3):75–79.

24. Thiel V, Ivanov KA, Putics Á. et al. *J.GenViro*, 2003; **84(9)**:2305–2315.
25. Wong G, BiY H, Wang QH, Chen XW, Zhang ZG, Yao YG. *Zool Res*, 2020; **41(3)**:213–219.
26. Wu C, Liu Y, Yang Y, Zhang P, Zhong W, Wang Y. et al. *Acta Pharm. Sin*, 2020; **10(5)**:766–788.
27. Xavier GS, Michael S. *IJARCSSE*, 2015; **5**:75-79.
28. Yang H, Yang M, Ding Y. et al. *PNAS*, 2003; **100(23)**:13190–13195.
29. Zhang C, Huang S, Zheng F, Dai Y. *J.Med. Viro*, 2020; **92(9)**:1441-1448.